

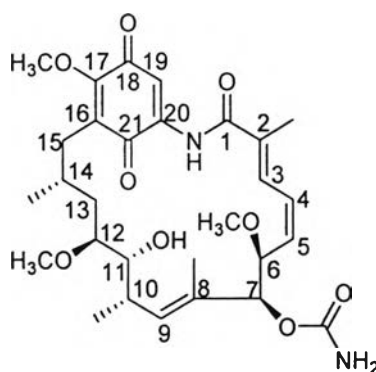


CHAPTER IV

RESULTS AND DISCUSSION

1. Chemical modification of geldanamycin

Derivatization of geldanamycin (1) was done mainly in the quinone moiety as follows:



Geldanamycin (1)

1.1 Modification of 17-OCH₃ into other alkoxy derivatives: 17-*O*-ethyl-17-*O*-demethylgeldanamycin (6), 17,19-di-*O*-ethyl-17-*O*-demethylgeldanamycin (7), 17-*O*-*n*-propyl-17-*O*-demethylgeldanamycin (8), and 17-*O*-benzyl-17-*O*-demethylgeldanamycin (9).

1.2 Modification of 17-OCH₃ into alkylamino derivatives: 17-amino-17-demethoxygeldanamycin (10), 17,19-di-methylamino-17-demethoxygeldanamycin (11), 17-ethylamino-17-demethoxygeldanamycin (12), 17-*n*-propylamino-17-demethoxygeldanamycin (13), 17,19-di-*n*-propylamino-17-demethoxygeldanamycin (14), 17-allylamino-17-demethoxygeldanamycin (15), 17,19-di-hydroxypropylamino-17-demethoxygeldanamycin (16), and 17-benzylamino-17-demethoxygeldanamycin (17).

1.3 Modification at C-19: 19-*O*-methylgeldanamycin (18), 19-aminogeldanamycin (19), and 19-glutathionylgeldanamycin (20).

1.4 Modification of 11-OH into other alkoxy derivatives: 11-*O*-methylgeldanamycin (21) and 11-*O*-acetylgeldanamycin (22).

1.5 Reduction of double bond at C-2 to C-5: 2,3,4,5-tetrahydrogeldanamycin (23).

According to geldanamycin (**1**) (Tadtong, 2000), the $^1\text{H-NMR}$ spectrum showed characteristic peaks of the olefinic protons at H-3 (δ 6.90 ppm, d), H-4 (δ 6.53 ppm, t), H-5 (δ 5.83 ppm, t), and H-9 (δ 5.77 ppm, d); the oxygenated protons at H-11 (δ 3.48 ppm, m), 17-OCH₃ (δ 4.08 ppm, s), and H-19 (δ 7.22 ppm, s). The $^{13}\text{C-NMR}$ spectrum presented characteristic peaks in quinone moiety of C-16 (δ 127.42 ppm), C-17 (δ 156.75 ppm), 17-OCH₃ (δ 61.71 ppm), C-18 (δ 183.88 ppm), C-19 (δ 111.63 ppm), C-20 (δ 137.86 ppm), and C-21 (δ 184.70 ppm). Modification of **1** was intensively observed the alteration of chemical shift at these positions which was further discussed in details below.

Comparison with the UV spectrum of geldanamycin (**1**), the UV spectra of the modified compounds showed the different characteristic spectra in each type of substituted group at quinone chromophore.

1. The 17-alkoxy substituted geldanamycins exhibited the similar UV absorption pattern to that of **1** which showed maxima absorption at λ_{max} 247 and 322 nm, however, longer alkoxy side chain possessed hyperchromic shift at λ_{max} 247 nm.

2. Replacement of oxygen atom with nitrogen atom at C-17 position possessed bathochromic shift at λ_{max} 322 nm to 332 nm and longer alkylamino side chain also exhibited greater UV absorption at this wavelength.

3. The disubstituted alkoxygeldanamycins at positions C-17 and C-19 expressed bathochromic shift (red shift) at λ_{max} 247 and 322 nm to 266 and 331 nm, respectively.

4. The disubstituted alkylaminogeldanamycins at positions C-17 and C-19 showed bathochromic shift at λ_{max} 247 and 322 nm to λ_{max} 254 and 343 nm, respectively.

5. The hydroquinone type geldanamycin revealed the maximum absorption only at λ_{max} 327 nm.

6. Reduction of double bond at C-2 to C-5 positions in ansa ring caused hypsochromic shift at λ_{max} 322 nm to 304 nm and underwent hypochromic shift at this wavelength and λ_{max} 247 nm.

The exact mass of the modified compounds from ESI-Q-TOF MS showed that the 17-substituted geldanamycins, 2,3,4,5-tetrahydrogeldanamycin (**23**), possessed

psuedomolecular ion peak at m/z $[M+Na]^+$ while the 19-substituted geldanamycins and 17,19-disubstituted geldanamycins presented the psuedomolecular ion peak at m/z $[M+Na+2H]^+$, which the quinone moiety might undergo reduction in ion source of mass spectrometer (Morisaki *et al.*, 1996; Sasaki *et al.*, 1970). However, only 19-glutathionylgeldanamycin (**20**) exhibited psuedomolecular ion peak at m/z $[M+H]^+$ in mass spectrum.

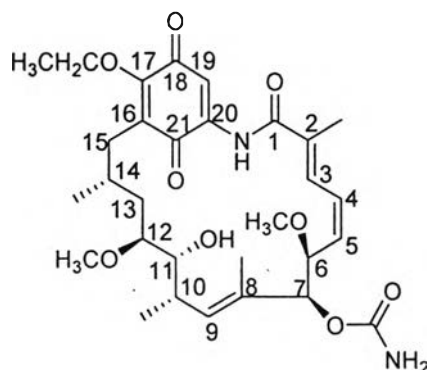
1.1 Modification of 17-OCH₃ into other alkoxy derivatives

1.1.1 17-O-ethyl-17-O-demethylgeldanamycin (**6**)

Geldanamycin (**1**) was converted to 17-*O*-ethyl-17-*O*-demethylgeldanamycin (**6**) in 72.20% yield by dissolving **1** in EtOH:DMSO and reacted with EtONa solution in DMSO. The ¹³C-NMR of **6** revealed two quinone carbonyl carbon signals at δ_C 184.00 (C-18) and 184.73 (C-21) which can deduce as quinone type geldanamycin derivative. The major difference form **1** was observed according to the absence of 17-OCH₃ (δ_C 61.71 and δ_H 4.08) and the presence of the -OCH₂CH₃ signal at δ_C 70.24 and δ_H 4.44 of -OCH₂CH₃, and δ_C 16.17 and δ_H 1.34 of -OCH₂CH₃ group (Figures D3, D4).

The absence of 17-OCH₃ signal in both of ¹³C- and ¹H-NMR spectra showed that the methoxyl group was displaced by the ethoxyl group in quinone moiety of **1**. This compound showed pseudomolecular ion peak $[M+Na]^+$ at m/z 597.2791 (Figure D1) which was calculated for C₃₀H₄₂N₂O₉Na at m/z 597.2783. This ESI-Q-TOFMS data represented 14 amu larger than **1**. The chemical structure of **6** was determined as the 17-*O*-ethyl-17-*O*-demethylgeldanamycin.

The UV spectrum of the compound (Figure D2) showed similar pattern to that of **1** (Figure A2) presenting the maximum absorption at λ_{max} (log ϵ) 247 nm (4.055), and 322 nm (4.033).



17-*O*-ethyl-17-*O*-demethylgeldanamycin (6)

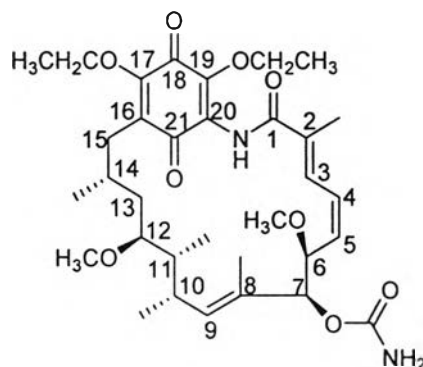
1.1.2 17, 19-di-*O*-ethyl-17-*O*-demethylgeldanamycin (7)

Compound 7 was obtained in 14.93% yield by the reaction of 1 with 2 equivalences of EtONa. According to the $^1\text{H-NMR}$ data of the compound, the absence of the singlet proton signal at δ_{H} 4.08 and the singlet proton signal at δ_{H} 7.22 was the major difference from that of 1, suggesting that the reaction was occurred at both positions of C-17 and C-19 in the quinone moiety of 1. The presence of two oxygenated methylene proton signals at δ_{H} 4.40 and 4.21 and two methyl proton signals at δ_{H} 1.33 and 1.29 of two $-\text{OCH}_2\text{CH}_3$ groups appeared in the $^1\text{H-NMR}$ spectrum instead (Figure E3). Due to limited amount of this compound, the $^{13}\text{C-NMR}$ data was not measured.

The pseudomolecular ion peak from ESI-Q-TOFMS presented $[\text{M}+\text{Na}+2\text{H}]^+$ at m/z 643.3115 (Figure E1) which was calculated for $\text{C}_{32}\text{H}_{48}\text{N}_2\text{O}_{10}\text{Na}$ at m/z 643.3201. Since it has been known that some quinones could yield apparent $\text{M}^+ + 2$ peaks in the ion source of the mass spectrometer (Morisaki *et al.*, 1996; Sasaki *et al.*, 1970), the chemical structure of this compound was determined as the 17,19-*O*-diethyl-17-*O*-demethylgeldanamycin (7) from the data described above and comparison to that of 1.

The UV spectrum of the compound (Figure E2) presented the maximum absorption at λ_{max} 266 nm (3.829), 331 nm (2.929), and 523 nm (2.176), the bathochromic shift from λ_{max} 247 to λ_{max} 266 was observed. However, the UV absorption pattern of this compound was similar to that of the quinone type,

geldanamycin (**1**) (Figure A2), and 17-*O*-demethylgeldanamycin (**2**) (Figure B2) and was different from that of 17-*O*-demethylgeldanamycin hydroquinone (**5**) (Figure C2).



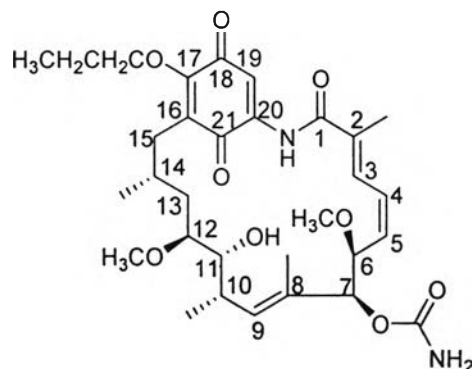
17,19-*O*-diethyl-17-*O*-demethylgeldanamycin (**7**)

1.1.3 17-*O*-*n*-propyl-17-*O*-demethylgeldanamycin (**8**)

Compound **8** in 73.33 % yield was converted from **1** reacted with *n*-PrONa solution in DMSO. The ^{13}C -NMR of **8** exhibited two quinone carbonyl carbon signals at δ_{C} 184.02 (C-18) and 184.70 (C-21) represented quinone type geldanamycin derivative. The absence of 17- OCH_3 signal at δ_{C} 61.71 and δ_{H} 4.08 and the presence of the $-\text{OCH}_2\text{CH}_2\text{CH}_3$ signal at δ_{C} 72.69 ppm, δ_{H} 4.36 ppm of $-\text{OCH}_2\text{CH}_2\text{CH}_3$; two additional signals at δ_{C} 23.95, δ_{H} 1.21 of $-\text{OCH}_2\text{CH}_2\text{CH}_3$; and δ_{C} 10.45, δ_{H} 1.00 of $-\text{OCH}_2\text{CH}_2\text{CH}_3$ (Figures F3, F4).

The reaction was occurred at position C-17 according to the absence of 17- OCH_3 signal in both of ^{13}C - and ^1H -NMR spectra. The methoxyl group was displaced by the propoxyl group in quinone moiety of **1**. The pseudomolecular ion peak of this compound was shown as $[\text{M}+\text{Na}]^+$ at m/z 611.2955 (Figure F1) which calculated for $\text{C}_{31}\text{H}_{44}\text{N}_2\text{O}_9\text{Na}$ at m/z 611.2939. The ESI-Q-TOFMS data revealed the 28 amu greater than **1**, then, chemical structure of this compound was deduced as the 17-*O*-*n*-propyl-17-*O*-demethylgeldanamycin (**8**) from the data described above and comparison to that of **1**.

The UV spectrum of the compound (Figure F2) presented the maximum absorption at λ_{\max} 246 nm (4.176) and 316 nm (4.099) which was similar to that of **1** (Figure A2). The chemical structure of **8** was shown below.



17-*O*-*n*-propyl-17-*O*-demethylgeldanamycin (**8**)

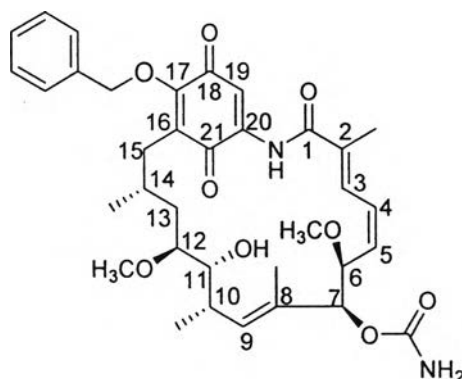
1.1.4 17-*O*-benzyl-17-*O*-demethylgeldanamycin (**9**)

Geldanamycin (**1**) was converted to **9** in 73.95% yield by dissolving **1** in BnOH:DMSO and reacted with BnONa solution in DMSO. Compound **9** showed two quinone carbonyl carbon signals at δ_{C} 184.05 (C-21) and 184.51 (C-18) in ^{13}C -NMR spectrum, represented quinone type geldanamycin derivative. The absence of 17- OCH_3 group at δ_{C} 61.71, δ_{H} 4.08 was replaced by the $-\text{OCH}_2\text{C}_6\text{H}_5$ group at δ_{C} 72.69 ppm, δ_{H} 5.35 of $-\text{OCH}_2\text{C}_6\text{H}_5$; δ_{C} 140.63, 129.13, 129.13, 128.34, 127.65 and 127.65, δ_{H} 7.20, 5H of $-\text{OCH}_2\text{C}_6\text{H}_5$ (Figures G3, G4).

The reaction was occurred at position C-17 because of the absence of 17- OCH_3 signal in both of ^{13}C -NMR and ^1H -NMR spectra. The replacement of the methoxyl group with the $-\text{OCH}_2\text{C}_6\text{H}_5$ group at position C-17 in quinone moiety of **1** was concluded. The ESI-Q-TOF MS showed the exact mass of this compound $[\text{M}+\text{Na}]^+$ at m/z 659.2971 (Figure G1) which was calculated for $\text{C}_{35}\text{H}_{44}\text{N}_2\text{O}_9\text{Na}$ at m/z 659.2939. The chemical structure of this compound was determined as the 17-*O*-benzyl-17-*O*-demethylgeldanamycin (**9**).

The UV spectrum of the compound (Figure G2) presented the maximum absorption at λ_{\max} 247 (3.860) nm and 329 nm (3.067) which possessed similar pattern to that of **1** (Figure A2) but reduced in UV absorption at both

wavelengths and the bathochromic shift was observed at wavelength of λ_{\max} 322 nm to 329 nm.



17-*O*-benzyl-17-*O*-demethylgeldanamycin (**9**)

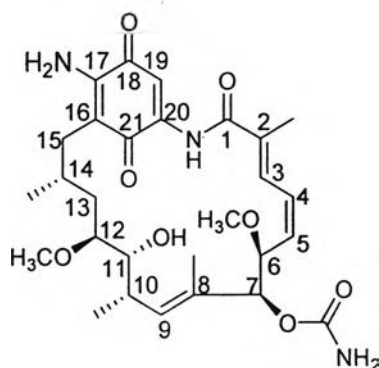
1.2 Modification of 17-OCH₃ into alkylamino derivatives

1.2.1 17-amino-17-demethoxygeldanamycin (**10**)

Modification of geldanamycin (**1**) into **10** in 68.48 % yield was performed by dissolving **1** in DMF and reacted with 10 equivalences of 70% NH₃ solution. The ¹³C-NMR of **10** expressed two quinone carbonyl carbon signals at δ_C 183.06 (C-18) and 180.40 (C-21) which was the quinone type geldanamycin derivative. The absence of 17-OCH₃ signal at δ_C 61.71, δ_H 4.08 was a major difference from that of **1**. Moreover, the upfield shift of the carbon signals of C-17 from δ_C 156.75 to δ_C 145.93 and C-16 from δ_C 127.42 to δ_C 110.25 was also observed in the ¹³C-NMR spectrum (Figure H4). The presence of the 17-NH₂ proton signal at δ_H 4.89 was also observed in ¹H-NMR spectrum (Figure H3).

According to the data mentioned above revealed that the reaction was occurred at position C-17, the methoxyl group was replaced by the amino group in quinone moiety of **1**. This compound showed pseudomolecular ion peak [M+Na]⁺ at m/z 568.3027 (Figure H1) which was calculated for C₂₈H₃₉N₃O₈Na at m/z 568.2635, represented the replacement of methoxy group with amino group. The chemical structure of this compound was determined as the 17-amino-17-demethoxygeldanamycin (**10**).

The chemical shift of two quinone carbonyl carbons was confirmed by HMBC correlation (Figure H5) exhibited the correlation between 1-NH (δ_{H} 9.11) to C-1 (δ_{C} 167.86), C-19 (δ_{C} 108.51), and C-21 (δ_{C} 180.40); H-15 (δ_{H} 2.73, 1.99) to 14-CH₃ (δ_{C} 23.72), C-16 (δ_{C} 110.25), and C-17 (δ_{C} 145.93); and H-19 (δ_{H} 7.28) to C-17 (δ_{C} 145.93), C-20 (δ_{C} 140.37), and C-21 (δ_{C} 180.40).



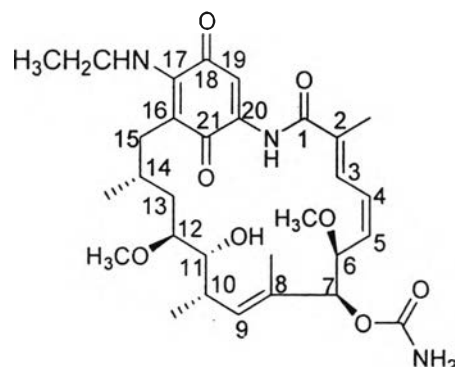
17-amino-17-demethoxygeldanamycin (**10**)

The UV spectrum of the compound (Figure H2) showed similar pattern to that of **1** (Figure A2) which presented the maximum absorption at λ_{max} (log ϵ) 246 nm (4.035) and 329 nm (4.300). The bathochromic shift was observed at the wavelength of 322 nm to 329 nm.

1.2.2 17,19-di-methylamino-17-demethoxygeldanamycin (**11**)

Geldanamycin (**1**) was dissolved in DMF and reacted with 1 equivalence of methylamine to give **11** (81.90% yield). The ¹³C-NMR of **11** exhibited two quinone carbonyl carbon signals at δ_{C} 183.76 (C-18) and 180.91 (C-21), which was quinone type geldanamycin derivative. The absence of signal at δ_{C} 61.71, δ_{H} 4.08 (17-OCH₃), and the signal at δ_{H} 7.22 (H-19) was observed in ¹³C-NMR and ¹H-NMR spectra of **11** showed that the reaction was occurred at positions C-17 and C-19 (Figures I3, I4). The presence of the equivalent nitrogenated carbon signal at δ_{C} 47.72, two nitrogenated methyl proton signals δ_{H} 3.15 and δ_{H} 2.84; and two NH proton signals at δ_{H} 6.84 and δ_{H} 6.68, were the signals of two -NHCH₃ groups. Moreover, the upfield shift of the carbon signals of C-17 from δ_{C} 156.75 to δ_{C} 141.17

shift of the carbon signal of C-17 from δ_C 156.75 to δ_C 144.81, the upfield shift of C-16 δ_C 127.42 to δ_C 108.35 was also observed. The chemical structure of **12** was deduced as 17-ethylamino-17-demethoxygeldanamycin.



17-ethylamino-17-demethoxygeldanamycin (**12**)

The compound showed pseudomolecular ion peak $[M+Na]^+$ at m/z 596.3008 (Figure J1) which was calculated for $C_{30}H_{43}N_3O_8Na$ at m/z 596.2948, represented the replacement of methoxy group with ethylamino group.

The UV spectrum of the compound (Figure J2) showed similar pattern to that of **1** (Figure A2) which presented the maximum absorption at λ_{max} 245 nm (4.163), 332 nm (4.340) and 527 nm (2.602). The bathochromic shift was observed at the wavelength of 322 nm to 332 nm.

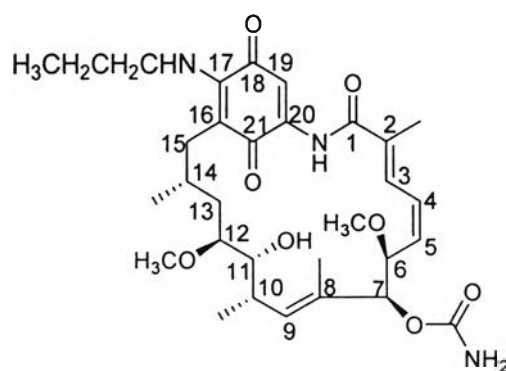
The HMBC correlation (Figure J5) revealed the correlation between 1-NH (δ_H 9.17) to C-1 (δ_C 168.38), C-19 (δ_C 108.64), and C-21 (δ_C 181.67); H-15 (δ_H 2.68, 2.40) to 14-CH₃ (δ_C 22.83), C-16 (δ_C 108.35), and C-17 (δ_C 144.81); 17-NHCH₂CH₃ (δ_H 6.20) to C-16 (δ_C 108.35), C-18 (δ_C 183.87), and 17-NHCH₂CH₃ (δ_C 15.12); 17-NHCH₂CH₃ (δ_H 3.62, 3.45) to C-17 (δ_C 144.81), and 17-NHCH₂CH₃ (δ_C 15.12); 17-NHCH₂CH₃ (δ_H 1.31) to 17-NHCH₂CH₃ (δ_C 40.66); and H-19 (δ_H 7.25) to C-17 (δ_C 144.81), C-20 (δ_C 141.43), and C-21 (δ_C 181.67).

1.2.4 17-n-propylamino-17-demethoxygeldanamycin (13)

Compound **13** was obtained in 72.52% yield by dissolving **1** in CH_2Cl_2 and reacted with 1 equivalence of $\text{CH}_3\text{CH}_2\text{CH}_2\text{NH}_2$ for 10 min. The ^{13}C -NMR of **13** exhibited two quinone carbonyl carbon signals at δ_{C} 183.89 (C-18) and 180.59 (C-21) which was the quinone type geldanamycin derivative (Figure K4). The absence of 17-OCH₃ signal at δ_{C} 61.71, δ_{H} 4.08 and the presence of $-\text{NHCH}_2\text{CH}_2\text{CH}_3$ group at δ_{C} 47.56, δ_{H} 3.50 of $-\text{NHCH}_2\text{CH}_2\text{CH}_3$; and two additional signals at δ_{C} 22.85, δ_{H} 1.68 of $-\text{NHCH}_2\text{CH}_2\text{CH}_3$; and δ_{C} 11.25, δ_{H} 0.93 of $-\text{NHCH}_2\text{CH}_2\text{CH}_3$ (Figures K3, K4). In addition, the upfield shift of the carbon signal of C-17 from δ_{C} 156.75 to δ_{C} 144.94 and C-16 δ_{C} 127.42 to δ_{C} 108.33 and were also observed in the ^{13}C -NMR spectrum.

According to the data from ESI-Q-TOFMS, the compound showed pseudomolecular ion peak $[\text{M}+\text{Na}]^+$ at m/z 610.3177 (Figure K1) which calculated for $\text{C}_{31}\text{H}_{45}\text{N}_3\text{O}_8\text{Na}$ at m/z 610.3104, and possessed 14 amu higher than 17-ethylamino-17-demethoxygeldanamycin. The compound was designated as 17-n-propylamino-17-demethoxygeldanamycin (**13**).

The UV spectrum of the compound (Figure K2) exhibited the maximum absorption at 247 nm (4.169), 332 nm (4.359) and 528 nm (2.602). The bathochromic shift was observed at wavelength of 322 nm to 332 nm. The chemical structure of 17-n-propylamino-17-demethoxygeldanamycin (**13**) was shown below.



17-n-propylamino-17-demethoxygeldanamycin (**13**)

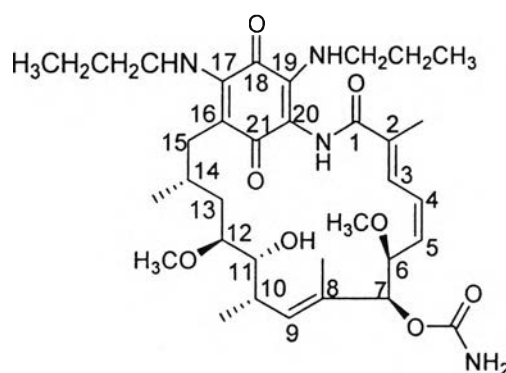
1.2.5 17,19-di-*n*-propylamino-17-demethoxygeldanamycin (14)

Geldanamycin (1) was dissolved in CH₂Cl₂ and reacted with 1 equivalence of CH₃CH₂CH₂NH₂ for 2 h to give 17,19-di-*n*-propylamino-17-demethoxygeldanamycin (14) in 81.84% yield. The ¹³C-NMR spectrum of 14 exhibited two quinone carbonyl carbon signals at δ_C 179.29 (C-18) and 179.01 (C-21) which was quinone type geldanamycin derivative (Figure L4). The absence of 17-OCH₃ signal at δ_C 61.71, δ_H 4.08 and H-19 at δ_H 7.22 ppm was observed in the ¹³C-NMR and ¹H-NMR spectra (Figures L3, L4). The presence of the two –NHCH₂CH₂CH₃ groups at δ_H 6.77 and δ_H 6.60 of –NHCH₂CH₂CH₃; two nitrogenated carbon and proton signals at δ_C 46.32 and δ_C 44.23, δ_H 3.45 and δ_H 3.07 of –NHCH₂CH₂CH₃; including four additional signals of –NHCH₂CH₂CH₃ at δ_C 23.62 and δ_C 21.60, four protons of two methylene groups at δ_H 1.65; and –NHCH₂CH₂CH₃ at δ_C 11.46, and δ_C 11.19, and six protons of two methyl groups at δ_H 0.95 was also observed in the ¹³C-NMR and ¹H-NMR spectra (Figures L3, L4). Moreover, the upfield shift of the carbon signals of C-17 from δ_C 156.75 to δ_C 147.50, C-16 from δ_C 127.42 to δ_C 91.91, and C-20 from δ_C 137.86 to δ_C 105.93, the downfield shift of C-19 from δ_C 111.63 to δ_C 150.74 were also observed in the ¹³C-NMR spectrum. The reaction was occurred at both positions of C-17 and C-19.

The pseudomolecular ion peak of this compound was shown as [M+Na+2H]⁺ *m/z* 669.3936 (Figure L1) which calculated for C₃₄H₅₄N₄O₈Na at *m/z* 669.3834. However, the data from ¹³C-NMR spectrum suggested that this compound was presented in quinone form and some quinones could yield apparent M⁺ + 2 peaks in the ion source of the mass spectrometer (Morisaki *et al.*, 1996; Sasaki *et al.*, 1970), then the chemical structure of this compound was determined as the 17,19-di-*n*-propylamino-17-demethoxygeldanamycin (14).

The UV spectrum of the compound (Figure L2) possessed the maximum absorption at λ_{max} 254 nm (4.415) and 346 nm (4.462) which showed the bathochromic shift at both wavelengths from that of 1 (Figure A2). The chemical structure of 14 was shown below.

The HMBC correlation (Figure L5) exhibited the correlation between H-15 (δ_H 2.41) to 14-CH₃ (δ_C 18.71), C-16 (δ_C 105.93), and C-17 (δ_C 147.50); 17-NHCH₂CH₂CH₃ (δ_H 6.77) to C-16 (δ_C 105.93), C-18 (δ_C 179.29), 17-NHCH₂CH₂CH₃ (δ_C 46.32), and 17-NHCH₂CH₂CH₃ (δ_C 23.62); 17-NHCH₂CH₂CH₃ (δ_H 3.45) to C-17 (δ_C 147.50), 17-NHCH₂CH₂CH₃ (δ_C 23.62), and 17-NHCH₂CH₂CH₃ (δ_C 11.19); 17-NHCH₂CH₂CH₃ (δ_H 1.65) to 17-NHCH₂CH₂CH₃ (δ_C 46.32) and 17-NHCH₂CH₂CH₃ (δ_C 11.19); 17-NHCH₂CH₂CH₃ (δ_H 0.95) to 17-NHCH₂CH₂CH₃ (δ_C 46.32) and 17-NHCH₂CH₂CH₃ (δ_C 23.62); 19-NHCH₂CH₂CH₃ (δ_H 6.60) to C-18 (δ_C 179.29), C-20 (δ_C 91.91), 19-NHCH₂CH₂CH₃ (δ_C 44.23), and 19-NHCH₂CH₂CH₃ (δ_C 21.60); 19-NHCH₂CH₂CH₃ (δ_H 3.07) to C-19 (δ_C 150.74), 19-NHCH₂CH₂CH₃ (δ_C 21.60), and 19-NHCH₂CH₂CH₃ (δ_C 11.46); 19-NHCH₂CH₂CH₃ (δ_H 1.65) to 19-NHCH₂CH₂CH₃ (δ_C 44.23) and 19-NHCH₂CH₂CH₃ (δ_C 11.46); and 19-NHCH₂CH₂CH₃ (δ_H 0.95) to 19-NHCH₂CH₂CH₃ (δ_C 44.23) and 19-NHCH₂CH₂CH₃ (δ_C 21.60).



17,19-di-n-propylamino-17-demethoxygeldanamycin (**14**)

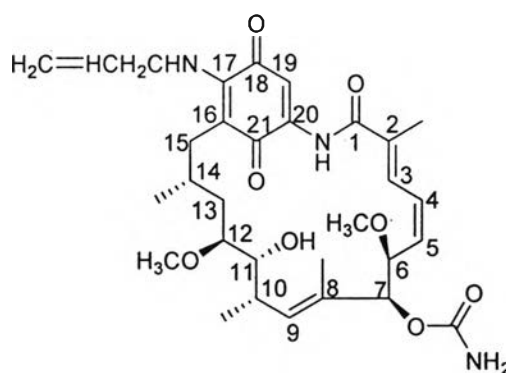
1.2.6 17-allylamino-17-demethoxygeldanamycin (**15**)

Compound **15** in the yield of 98.57% was performed by dissolving **1** in CH₂Cl₂ and reacted with 40 equivalences of allylamine. According to ¹³C-NMR data (Figure M4), **15** possessed two signals of quinone carbonyl carbon at δ_C 183.76 (C-18) and 180.91 (C-21). The absence of 17-OCH₃ signal at δ_C 61.71, δ_H 4.08 and the presence of the -NHCH₂CH=CH₂ at δ_H 6.37 of -NHCHCH₂=CH₂; δ_C 47.72, δ_H 3.81 of -NHCH₂CH=CH₂; δ_C 132.47, δ_H 5.92 of -NHCH₂CH=CH₂; and δ_C 118.46, δ_H 5.29 of -NHCH₂CH=CH₂ (Figures M3, M4). Moreover, the upfield shift of the carbon signals of C-17 from δ_C 156.75 to δ_C 144.61, and C-16 from δ_C 127.42

to δ_C 108.74 was examined. The chemical structure of **15** was determined as 17-allylamino-17-demethoxygeldanamycin.

The data from ESI-Q-TOFMS showed that this compound exhibited pseudomolecular ion peak $[M+Na]^+$ at m/z 608.3555 (Figure M1) which calculated for $C_{31}H_{43}N_3O_8Na$ at m/z 608.2948, and possessed 12 amu higher than 17-ethylamino-17-demethoxygeldanamycin (**12**). The 17-OCH₃ group of **1** was replaced by allylamino group in **15**.

The UV spectrum of the compound (Figure M2) possessed the maximum absorption at 244 nm (4.241), 332 nm (4.394) and 522 nm (2.477). The bathochromic shift was observed at wavelength of 322 nm to 332 nm. The chemical structure of **15** was shown below.



17-allylamino-17-demethoxygeldanamycin (**15**)

1.2.7 17,19-di-hydroxypropylamino-17-demethoxygeldanamycin (**16**)

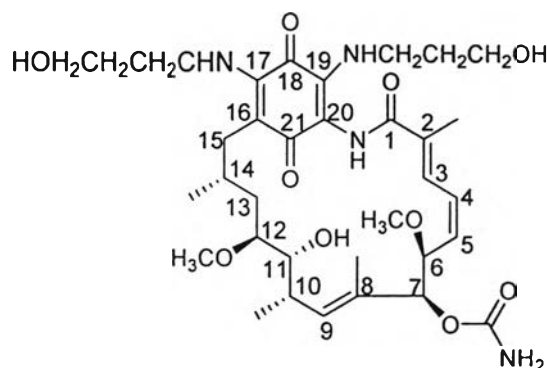
The solution of **1** in ACN was reacted with 1 equivalence of HOCH₂CH₂CH₂NH₂ to give **16** in 58.00%. Compound **16** showed the absence of 17-OCH₃ signal at δ_C 61.71, δ_H 4.08 and H-19 signal at δ_H 7.22 in the ¹³C-NMR and ¹H-NMR spectra exhibited that the reaction was occurred at positions C-17 and C-19 (Figures N3, N4). The presence of two -NHCH₂CH₂CH₂OH groups at δ_H 7.67 and δ_H 7.19 of -NHCH₂CH₂CH₂OH; δ_H 7.47 and δ_H 6.69 of -NHCH₂CH₂CH₂OH; δ_C 41.41 and δ_C 40.03, δ_H 4.36 and δ_H 3.15 of -NHCH₂CH₂CH₂OH; δ_C 58.58 and δ_C 58.58, δ_H 4.60 and δ_H 3.45 of -NHCH₂CH₂CH₂OH; and δ_C 32.70 and δ_C 30.53, δ_H 1.67 and δ_H 1.65 of -NHCH₂CH₂CH₂OH. The upfield shift of the carbon signals of

C-17 from δ_C 156.75 to δ_C 146.98, C-16 from δ_C 127.42 to δ_C 105.32, and C-20 from δ_C 137.86 to δ_C 91.06, the downfield shift of C-19 from δ_C 111.63 to δ_C 150.47 were also observed in the ^{13}C -NMR spectrum.

The pseudomolecular ion peak of this compound was shown as $[\text{M}+\text{Na}+2\text{H}]^+$ m/z 701.3751 (Figure N1) which calculated for $\text{C}_{34}\text{H}_{54}\text{N}_4\text{O}_{10}\text{Na}$ at m/z 701.3732. However, the data from ^{13}C -NMR spectrum suggested that this compound was presented in quinone form at δ_C 178.36 (C-18) and δ_C 178.28 (C-21), and some quinones could yield apparent $\text{M}^+ + 2$ peaks in the ion source of the mass spectrometer (Morisaki *et al.*, 1996; Sasaki *et al.*, 1970), then the chemical structure of this compound was designated as the 17,19-di-hydroxypropylamino-17-demethoxygeldanamycin (**16**).

The UV spectrum of the compound (Figure N2) possessed the maximum absorption at λ_{max} 251 nm (4.502) and 343 nm (4.389) which showed the bathochromic shift at both wavelengths from that of **1** (Figure A2). The chemical structure of **16** was shown below.

The HMBC correlation (Figure N5) exhibited the correlation between 17-NHCH₂CH₂CH₂OH (δ_H 7.19) to C-16 (δ_C 105.32), C-18 (δ_C 178.36), and 17-NHCH₂CH₂CH₂OH (δ_C 41.41); 17-NHCH₂CH₂CH₂OH (δ_H 3.47) to C-17 (δ_C 147.50), 17-NHCH₂CH₂CH₂OH (δ_C 32.70), and 17-NHCH₂CH₂CH₂OH (δ_C 58.36); 17-NHCH₂CH₂CH₂OH (δ_H 1.65) to 17-NHCH₂CH₂CH₂OH (δ_C 41.41) and 17-NHCH₂CH₂CH₂OH (δ_C 58.36); 17-NHCH₂CH₂CH₂OH (δ_H 4.60) to 17-NHCH₂CH₂CH₂OH (δ_C 41.41); 19-NHCH₂CH₂CH₂OH (δ_H 7.67) to C-18 (δ_C 178.36), C-20 (δ_C 91.06), and 19-NHCH₂CH₂CH₂OH (δ_C 40.03); 19-NHCH₂CH₂CH₂OH (δ_H 3.15) to C-19 (δ_C 150.47), 19-NHCH₂CH₂CH₂OH (δ_C 30.53), and 19-NHCH₂CH₂CH₂OH (δ_C 58.58); 19-NHCH₂CH₂CH₂OH (δ_H 1.67) to 19-NHCH₂CH₂CH₂OH (δ_C 40.03) and 19-NHCH₂CH₂CH₂OH (δ_C 58.58); and 19-NHCH₂CH₂CH₂OH (δ_H 3.45) to 19-NHCH₂CH₂CH₂OH (δ_C 40.03).

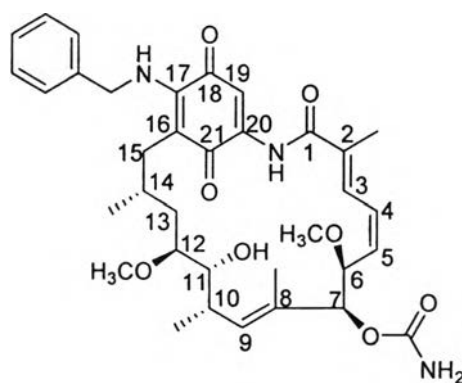


17,19-di-hydroxypropylamino-17-demethoxygeldanamycin (**16**)

1.2.8 17-benzylamino-17-demethoxygeldanamycin (**17**)

Geldanamycin (**1**) in CH_2Cl_2 was reacted with 10 equivalents of benzylamine to yield **17** in 68.06%. Compound **17** showed two quinone carbonyl carbon signals at δ_{C} 183.72 (C-18) and 180.99 (C-21), expressed quinone type geldanamycin derivative in the ^{13}C -NMR spectrum (Figure O4). The absence of 17- OCH_3 signal at δ_{C} 61.71, δ_{H} 4.08 was replaced by and the $-\text{NHCH}_2\text{C}_6\text{H}_5$ group at δ_{C} 50.04, and δ_{H} 4.75 and 4.61 of nonequivalent protons of $-\text{NHCH}_2\text{C}_6\text{H}_5$; δ_{C} 129.13, δ_{C} 127.65, δ_{C} 128.34, and five protons at δ_{H} 7.29 of $-\text{NHCH}_2\text{C}_6\text{H}_5$ (Figures O3, O4).

The ESI-Q-TOF MS showed the exact mass of this compound $[\text{M}+\text{Na}]^+$ at m/z 658.3829 (Figure O1) which was calculated for $\text{C}_{35}\text{H}_{45}\text{N}_3\text{O}_8\text{Na}$ at m/z 658.3104. The chemical structure of this compound was determined as the 17-benzylamino-17-demethoxygeldanamycin (**17**).



17-benzylamino-17-demethoxygeldanamycin (**17**)

The UV spectrum of the compound (Figure O2) presented the maximum absorption at λ_{\max} 254 nm (4.380), 333 nm (4.422) and 530 nm (2.699) which the bathochromic shift was observed at all wavelengths.

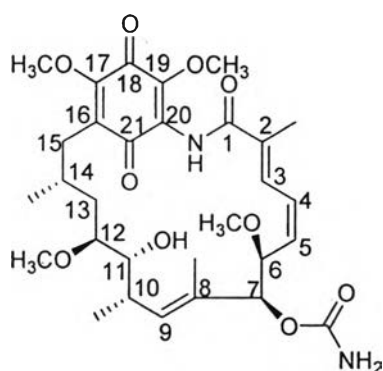
1.3 Modification at C-19 position

1.3.1 19-*O*-methylgeldanamycin (18)

Geldanamycin (**1**) was converted to **18** in 73.14% yield by dissolving **1** in MeOH and reacted with 2 equivalences of MeONa. Intensively analysis of ^{13}C -NMR data, compound **18** possessed two signals of quinone carbonyl carbon at δ_{C} 181.99 (C-18) and 183.75 (C-21) (Figure P4). The absence of H-19 at δ_{H} 7.22 and the additional methoxy carbon signal was observed at δ_{C} 52.10, δ_{H} 3.75 was the major difference to that of **1** (Figures P3, P4). Moreover, the downfield shift of the carbon signal of C-19 from δ_{C} 111.63 to δ_{C} 158.03 was examined in the ^{13}C -NMR spectrum suggested that the reaction was occurred at position C-19. The HMBC spectrum (Figure P5) exhibited the long range correlation between H-15 (δ_{H} 2.26) to C-17 (δ_{C} 158.03); 17-OCH₃ (δ_{H} 4.04) to C-17 (δ_{C} 158.03); and 19-OCH₃ (δ_{H} 3.75) to C-19 (δ_{C} 168.44).

The ESI-Q-TOFMS showed the pseudomolecular ion peak $[\text{M}+\text{Na}+2\text{H}]^+$ at m/z 615.2804 (Figure P1) which calculated for C₃₀H₄₄N₂O₁₀Na at m/z 615.2888. Since some quinones could yield apparent $\text{M}^+ + 2$ peaks in the ion source of the mass spectrometer (Morisaki *et al.*, 1996; Sasaki *et al.*, 1970), and in the ^{13}C -NMR spectrum exhibited quinone type geldanamycin derivative, the chemical structure of compound **18** was designated as 19-*O*-methylgeldanamycin.

The UV spectrum of the compound (Figure P2) possessed the maximum absorption at 266 nm (4.004), 307 nm (3.255) and 530 nm (2.602). The bathochromic shift was observed at wavelength of 247 nm to 266 nm and possessed hypsochromic shift at λ_{\max} 322 nm to 307 nm and reduced in UV absorption at this wavelength. The chemical structure of **18** was shown below.



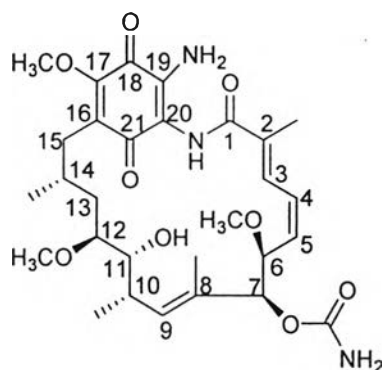
19-*O*-methylgeldanamycin (**18**)

1.3.2 19-aminogeldanamycin (**19**)

Modification of **1** into **19** in 73.03% yield was performed by dissolving **1** in MeOH and reacted with 2 equivalences of 70% NH₃ solution. The ¹³C-NMR of **19** expressed two quinone carbonyl carbon signals at δ_C 178.25 (C-18) and 178.87 (C-21) was the quinone type geldanamycin derivative. The downfield shift of the carbon signals at C-19 from δ_C 111.63 to δ_C 149.34 and the upfield shift of the carbon signals at C-16 and C-20 from δ_C 127.42 and δ_C 137.86, respectively, to δ_C 105.99 were also observed in the ¹³C-NMR spectrum (Figure Q4). The absence of singlet H-19 proton signal at δ_H 7.22 and the presence of the 19-NH₂ proton signal at δ_H 5.25 were examined in ¹H-NMR spectrum suggested that the reaction was occurred at position C-19 (Figure Q3).

The compound showed pseudomolecular ion peak [M+Na+2H]⁺ at m/z 600.3427 (Figure Q1) which was calculated for C₂₉H₄₃N₃O₉Na at m/z 600.2892. The chemical structure of this compound was determined as the 19-aminogeldanamycin (**19**).

The UV spectrum of the compound (Figure Q2) presented the maximum absorption at λ_{max} 260 nm (4.445) and 332 nm (4.497) which the bathochromic shift was observed at all wavelengths.

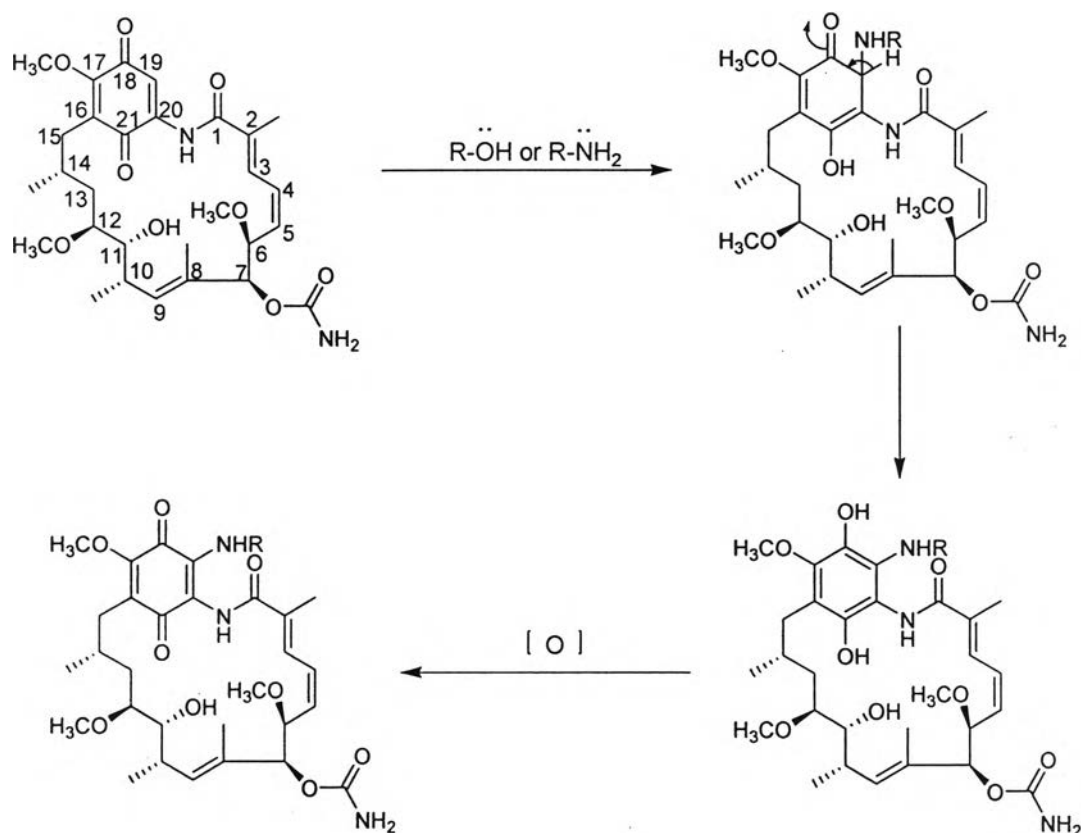
19-aminogeldanamycin (**19**)

1.3.3 19-glutathionylgeldanamycin (**20**)

The reaction was done by dissolved **1** in DMSO and reacted with 1 equivalence of glutathione to give **20** in 69.90%. The $^1\text{H-NMR}$ data of **20** showed the absence of singlet H-19 proton signal at δ_{H} 7.22 ppm was a major difference from that of **1**, which was revealed that the reaction occurred at position C-19 of **1**. The presence of glutathione (Gly-Cys-Glu) proton signals, three α -proton signals of three amino acids, Cys at δ_{H} 4.25, Gly at δ_{H} 3.95, and Glu at δ_{H} 3.45; -SCH₂- proton signal of Cys at δ_{H} 3.6; two methylene proton signals of Glu at δ_{H} 2.08 and δ_{H} 1.75; and -NH₂ proton signal of Glu at δ_{H} 8.64 ppm represented that position C-19 of **1** reacted with sulfur molecule of glutathione (Figure R3).

The pseudomolecular ion peak from ESI-Q-TOFMS presented $[\text{M}+\text{H}]^+$ at m/z 866.3986 (Figure R1) which was calculated for C₃₉H₅₆N₅O₁₅S at m/z 866.3494. This compound was determined as 19-glutathionylgeldanamycin (**20**).

The UV spectrum of the compound (Figure R2) presented the maximum absorption at λ_{max} 256 nm (4.172) and 329 nm (2.301) the bathochromic shift of both wavelengths were observed.



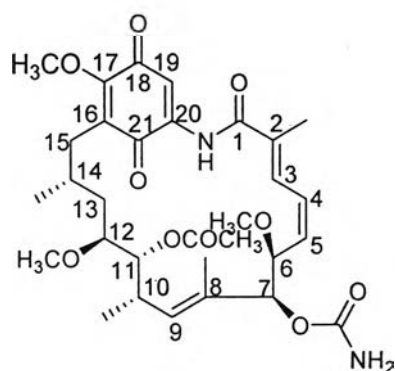
Scheme 2. Reaction mechanism of 19-substituted geldanamycins.

1.4 Modification of 11-OH into other alkoxy derivatives:

1.4.1 11-*O*-methylgeldanamycin (21)

Geldanamycin (**1**) was dissolved in DMF and reacted with 4 equivalences of anhydrous potassium carbonate and methyl iodide to yield **21** in 45.51%. Compound **21** showed two quinone carbonyl carbon signals at δ_C 182.65 ppm (C-18) and 182.46 (C-21) which was the quinone type geldanamycin derivative (Figure S3). The extra -OCH₃ signal at δ_C 56.58, δ_H 3.34 ppm was observed (Figures S2, S3). In addition, the downfield shift of H-11 from δ_H 3.48 ppm to δ_H 3.60 ppm (Figure S2), which indicated that the reaction was occurred at position C-11 to yield 11-*O*-methylgeldanamycin (**21**).

The HRFABMS presented that the compound possessed pseudomolecular ion peak $[M+Na+2H]^+$ at m/z 599.2925 which was calculated for C₃₀H₄₄N₂O₉Na at m/z 599.2939. However, the quinone carbonyl carbons were

11-*O*-acetylgeldanamycin (**22**)

1.5 Reduction of double bond at C-2 to C-5 positions:

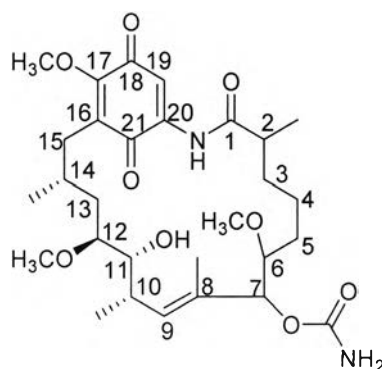
1.5.1 2,3,4,5-tetrahydrogeldanamycin (**23**)

Geldanamycin was converted to **23** in 43.69% yield by dissolving in MeOH and reacted with H₂ gas in normal atmosphere and 10% PdC was used as catalyst. The ¹H-NMR spectrum of **23** showed that olefinic proton signals at positions H-3 (δ_{H} 6.90, 1H), H-4 (δ_{H} 6.53, 1H), and H-5 (δ_{H} 5.83, 1H) were disappeared. However, four more sp³ proton signals of H-2 (δ_{H} 2.42, 1H), H-3 (δ_{H} 1.65, 2H), H-4 (δ_{H} 1.40, 2H), and H-5 (δ_{H} 1.50, 2H) were detected in the ¹H-NMR spectrum, indicated that the olefinic carbons at position C-2, C-3, C-4, and C-5 underwent reduction to yielded 2,3,4,5-tetrahydrogeldanamycin (**23**).

Moreover, the 2-CH₃ proton signal exhibited upfield shift from δ_{H} 1.98 ppm to the two different 2-CH₃ proton signals at δ_{H} 1.22 and δ_{H} 1.18 which supported that the reduction reaction was occurred at C-2 to C-5 position of geldanamycin molecule to give the different conformation of 2-CH₃. In addition, two sets of proton signals of 1-NH at δ_{H} 8.76 ppm and δ_{H} 8.41 ppm, and 2-CH₃ at δ_{H} 1.22 ppm and δ_{H} 1.18 ppm were also observed in the spectrum (Figure U3), which suggested that the reaction products contained two diastereomers of 2,3,4,5-tetrahydrogeldanamycin (**23**). According to intensity of 1-NH peaks, mixture was presented in 1:1 ratio and cannot isolate into single isomer.

The ESI-Q-TOFMS exhibited the pseudomolecular ion peak $[M+Na]^+$ at m/z 587.2928 (Figure U1) calculated for $C_{29}H_{44}N_2O_{10}Na$ at m/z 587.2939 which showed 4 amu greater than **1** designated as 2,3,4,5-tetrahydrogeldanamycin (**23**).

The UV spectrum revealed that the UV absorption occurred at λ_{max} 245 nm (2.653), 304 nm (3.720), 527 nm (2.699). The hypsochromic shift was observed at wavelength 322 nm to 307 nm (Figure U2). At all wavelengths the hypochromic shift was observed due to conjugated double bonds were reduced.



2,3,4,5-tetrahydrogeldanamycin (**23**)

2. Culture of P19 cells

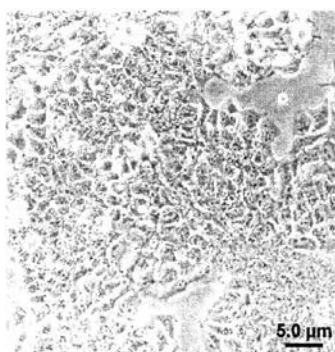


Figure 9. The exponentially grown monolayer P19 cells at 100 \times .

The exponentially grown P19 cells with fibroblast-like morphology (Figure 9) were cultured in α -MEM supplemented with 7.5% NCS and 2.5% FBS in a 5% CO_2 humidified atmosphere, at 37 $^{\circ}C$. P19 cells were maintained as monolayer and subcultured every 2 days.

3. P19 Neuron-like cells differentiation

For differentiation, exponentially grown cell cultures were trypsinized and dissociated into single cells. P19 cells (2×10^6 cells/mL) were then suspended in 10 mL α -MEM supplemented with 5% FBS and $0.5 \mu\text{M}$ RA and seeded onto a 100-mm bacteriological culture dish. The cells formed large aggregates or embryoid bodies in suspension after 3 days (Figure 10). After 4 days of the RA treatment, the aggregates were dissociated by a 5-mL glass measuring pipette and re-plated on poly-L-lysine-pre-coated 96-well plates at 7×10^4 cells/mL, in α -MEM supplemented with 10% FBS without RA and further incubated for 24 h. At day 1 after plating, cells changed in morphology appeared to have branching processes (Figure 11). Ara-C ($10 \mu\text{M}$) was added at day one after plating and the medium was changed every 2-3 days. The P19 NLCs reached maturing after day 8 of plating and contained long branching processes with rounded shape cells (Figure 12). The differentiated neuronal cells, P19 NLCs, were used after day 14 of the differentiation process.

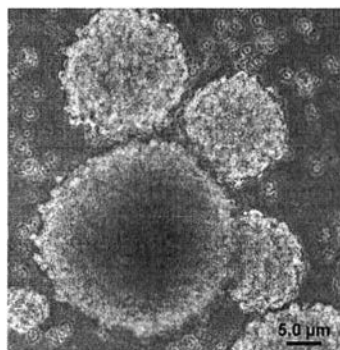


Figure 10. The 3 days old P19 embryoid bodies at 100 \times .

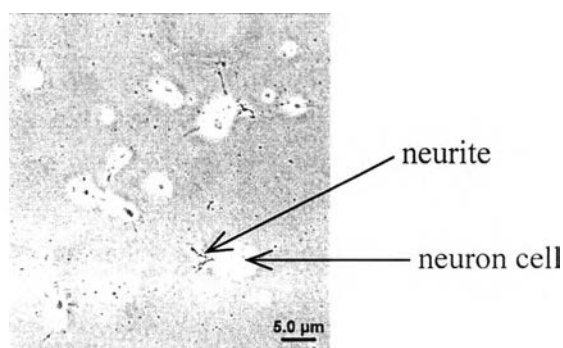


Figure 11. P19 NLCs at day 1 after plating, before adding $10 \mu\text{M}$ Ara-C at 100 \times .

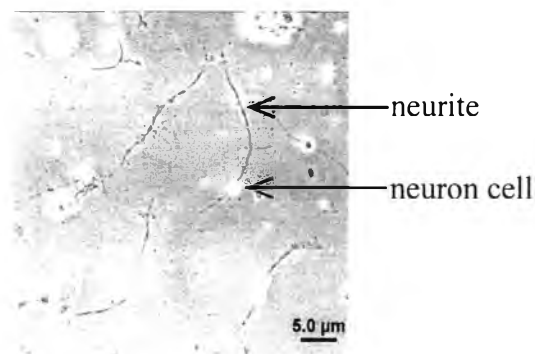


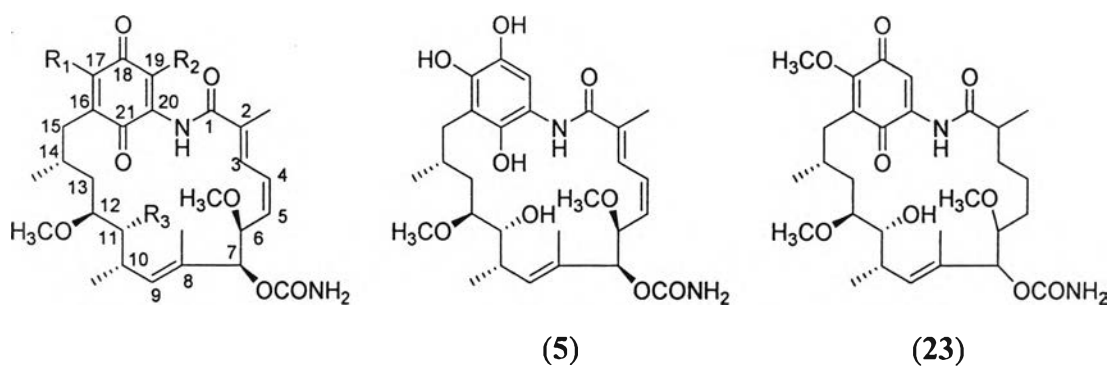
Figure 12. P19 NLCs at day 8 after plating at 100 \times .

All of the semisynthetic geldanamycin analogues mentioned in the previous section, as well as three natural occurring ansamycins, geldanamycin (**1**) 17-*O*-demethylgeldanamycin (**2**), and 17-*O*-demethylgeldanamycin hydroquinone (**5**), as shown in Figure 13, were investigated for biological activities on P19 cells and P19 NLCs as described in Chapter III.

4. Cytotoxic effect of geldanamycins on P19 cells

Due to limited amount of other geldanamycin derivatives, only geldanamycin (**1**) was subjected to evaluate the IC_{50} for cytotoxic activity on P19 cells. The results showed that geldanamycin (**1**) displayed cytotoxicity on P19 cells at IC_{50} of 0.1 μ M (Figure 14). Then, other derivatives were compared their cytotoxic activities to geldanamycin (**1**) at the concentration of 0.1 μ M.

Other geldanamycin derivatives were evaluated for their cytotoxicities on P19 cells at the same concentration of 0.1 μ M. The % cell viability from Table 4 showed that all of the compounds possessed less cytotoxicity on P19 cells than geldanamycin (**1**). These less cytotoxic compounds are suitable to be evaluated their neuritogenic and neurotoxicity on P19 NLCs.



Compound	R ₁	R ₂	R ₃
1	OCH ₃	H	OH
2	OH	H	OH
6	OCH ₂ CH ₃	H	OH
7	OCH ₂ CH ₃	OCH ₂ CH ₃	OH
8	OCH ₂ CH ₂ CH ₃	H	OH
9	OCH ₂ C ₆ H ₅	H	OH
10	NH ₂	H	OH
11	NHCH ₃	NHCH ₃	OH
12	NHCH ₂ CH ₃	H	OH
13	NHCH ₂ CH ₂ CH ₃	H	OH
14	NHCH ₂ CH ₂ CH ₃	NHCH ₂ CH ₂ CH ₃	OH
15	NHCH ₂ CH=CH ₂	H	OH
16	NHCH ₂ CH ₂ CH ₂ OH	NHCH ₂ CH ₂ CH ₂ OH	OH
17	NHCH ₂ C ₆ H ₅	H	OH
18	OCH ₃	OCH ₃	OH
19	OCH ₃	NH ₂	OH
20	OCH ₃	GS*	OH
21	OCH ₃	H	OCH ₃
22	OCH ₃	H	OCOCH ₃

*GS = glutathione (C₁₀H₁₆H₃O₆S)

Figure 13. Chemical structures of geldanamycin and its derivatives for biological activities evaluation.

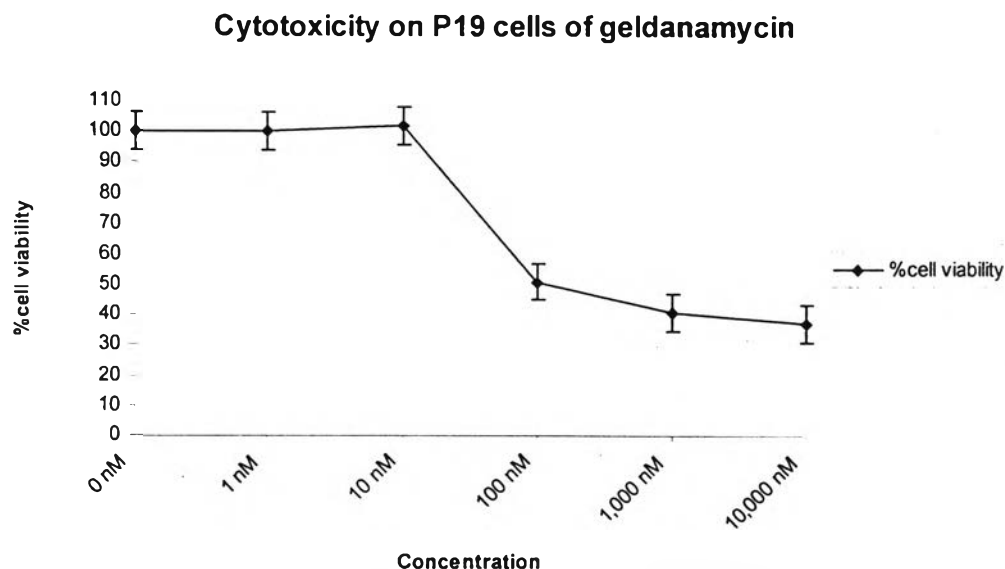


Figure 14. Cytotoxicity of geldanamycin (**1**) on P19 cells ($IC_{50} = 0.1 \mu M$).

The results from Table 4 showed that

1. The compounds with larger alkoxy substitution at C-17 (compounds **6**, **8**, and **9**) exhibited the less cytotoxicity on P19 cells.
2. The replacement of oxygen by nitrogen at C-17 (compounds **10**, **12**, **13**, **15**, and **17**) showed remarkably less cytotoxicity on P19 cells.
3. The C-17, C-19 disubstituted geldanamycins with smaller groups (compounds **11**, **18**, **19**) showed no cytotoxicity.
4. Modification at C-11 position caused dramatically lost in cytotoxicity of geldanamycin (**1**).
5. Reduction of double bonds at C-2 to C-5 positions in the ansa ring reduced the cytotoxic activity of geldanamycin (**1**).

The data suggested that the conjugated double bonds at C-2 to C-5 and the 11-OH are necessary for cytotoxic activity of geldanamycin.

Table 4. Percentage of cell viability of P19 cells when treated with geldanamycin and its derivatives at concentration of 0.1 μ M.

Compound	% Cell viability \pm SEM
Geldanamycin (1)	51 \pm 0.025
17- <i>O</i> -Demethylgeldanamycin (2)	83 \pm 0.009
17- <i>O</i> -Demethylgeldanamycin hydroquinone (5)	72 \pm 0.009
17- <i>O</i> -Ethyl-17- <i>O</i> -demethylgeldanamycin (6)	72 \pm 0.008
17- <i>O</i> - <i>n</i> -Propyl-17- <i>O</i> -demethylgeldanamycin (8)	77 \pm 0.005
17- <i>O</i> -Benzyl-17- <i>O</i> -demethylgeldanamycin (9)	101 \pm 0.008
17-Amino-17-demethoxygeldanamycin (10)	113 \pm 0.047
17-Ethylamino-17-demethoxygeldanamycin (12)	97 \pm 0.082
17- <i>n</i> -Propylamino-17-demethoxygeldanamycin (13)	95 \pm 0.028
17-Allylamino-17-demethoxygeldanamycin (15)	97 \pm 0.055
17-Benzylamino-17-demethoxygeldanamycin (17)	85 \pm 0.129
19- <i>O</i> -Methylgeldanamycin (18)	122 \pm 0.030
17,19-Di- <i>O</i> -ethyl-17- <i>O</i> -demethylgeldanamycin (7)	87 \pm 0.004
17,19-Di-methylamino-17-demethoxygeldanamycin (11)	111 \pm 0.067
17,19-Di- <i>n</i> -propylamino-17-demethoxygeldanamycin (14)	83 \pm 0.135
17,19-Di-hydroxypropylamino-17-demethoxygeldanamycin (16)	90 \pm 0.154
19-Aminogeldanamycin (19)	118 \pm 0.019
19-Glutathionylgeldanamycin (20)	99 \pm 0.301
11- <i>O</i> -Methylgeldanamycin (21)	85 \pm 0.007
11- <i>O</i> -Acetylgeldanamycin (22)	84 \pm 0.021
2,3,4,5-Tetrahydrogeldanamycin (23)	72 \pm 0.024

5. Neurotoxic activity of geldanamycins on P19 NLCs

All of the compounds were further investigated for their neurotoxic activity on P19 NLCs. However, due to limited amount of them, only geldanamycin (1) was subjected to determine for its neurotoxic activity on P19 NLCs by varying its

concentrations. Geldanamycin (**1**) displayed neurotoxicity on P19 NLCs at IC_{50} of 2.0 μ M. Interestingly, at the very low concentration of 1 nM, geldanamycin (**1**) promoted viability of P19 NLC at 169% (Figure 15).

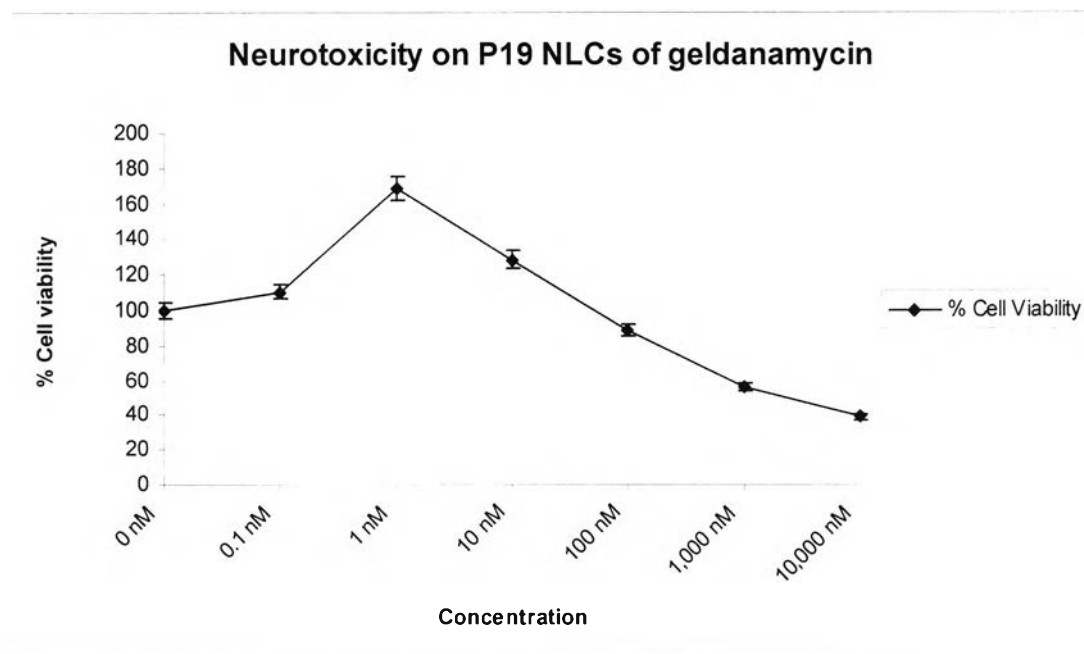


Figure 15. Neurotoxic activity of geldanamycin (**1**) on P19 NLCs (neurotoxicity at IC_{50} of 2.0 μ M, promoted viability of P19 NLCs at concentration of 1 nM).

Other geldanamycin derivatives were then comparatively evaluated for their bioactivity on P19 NLCs at a concentration of 1 nM. The results (Table 5) showed that most of the compounds displayed neurotoxicity on P19 NLCs at this concentration.

The results from Table 5 suggested that

1. The 17-*O*-alkyl-17-*O*-demethylgeldanamycins (compounds **6**, **8**, and **9**) possessed neuritogenic activity on P19 NLCs, however, they were less effective than geldanamycin (**1**).
2. The replacement of oxygen by nitrogen at C-17 (compounds **10**, **12**, **13**, **15**, and **17**) showed higher neurotoxicity on P19 NLCs.
3. The disubstituted geldanamycin with smaller group at C-17 and C-19 (compound **18**) showed less neurotoxicity than the larger one.
4. Modification at C-11 position promoted neurotoxicity of geldanamycin (**1**).

5. Reduction of double bonds at C-2 to C-5 positions in the ansa ring caused neurotoxicity on P19 NLCs.

Table 5. Percentage of cell viability of P19 NLCs when treated with geldanamycin and its derivatives at concentration of 1 nM.

Compound	% Cell viability \pm SEM
Geldanamycin (1)	169 \pm 0.060
17- <i>O</i> -Demethylgeldanamycin (2)	50 \pm 0.015
17- <i>O</i> -Demethylgeldanamycin hydroquinone (5)	43 \pm 0.007
17- <i>O</i> -Ethyl-17- <i>O</i> -demethylgeldanamycin (6)	113 \pm 0.003
17- <i>O</i> - <i>n</i> -Propyl-17- <i>O</i> -demethylgeldanamycin (8)	121 \pm 0.039
17- <i>O</i> -Benzyl-17- <i>O</i> -demethylgeldanamycin (9)	111 \pm 0.004
17-Amino-17-demethoxygeldanamycin (10)	85 \pm 0.005
17-Ethylamino-17-demethoxygeldanamycin (12)	49 \pm 0.005
17- <i>n</i> -Propylamino-17-demethoxygeldanamycin (13)	0 \pm 0.002
17-Allylamino-17-demethoxygeldanamycin (15)	66 \pm 0.008
17-Benzylamino-17-demethoxygeldanamycin (17)	44 \pm 0.060
19- <i>O</i> -Methylgeldanamycin (18)	108 \pm 0.003
17,19-Di- <i>O</i> -ethyl-17- <i>O</i> -demethylgeldanamycin (7)	0 \pm 0.002
17,19-Di-methylamino-17-demethoxygeldanamycin (11)	46 \pm 0.004
17,19-Di- <i>n</i> -propylamino-17-demethoxygeldanamycin (14)	0 \pm 0.030
17,19-Di-hydroxypropylamino-17-demethoxygeldanamycin (16)	0 \pm 0.030
19-Aminogeldanamycin (19)	91 \pm 0.005
19-Glutathionylgeldanamycin (20)	32 \pm 0.005
11- <i>O</i> -Methylgeldanamycin (21)	68 \pm 0.018
11- <i>O</i> -Acetylgeldanamycin (22)	55 \pm 0.016
2,3,4,5-Tetrahydrogeldanamycin (23)	72 \pm 0.004

In contrast, geldanamycin (1); the 17-alkoxy analogues, including 17-*O*-ethyl-17-*O*-demethyl-geldanamycin (6), 17-*O*-*n*-propyl-17-*O*-demethylgeldanamycin (8), and 17-

O-benzyl-17-*O*-demethyl-geldanamycin (**9**); and the disubstituted geldanamycin, 19-*O*-methyl-geldanamycin (**18**), promoted viability of P19 NLCs when observed by XTT reduction assay at this concentration. Then these four compounds were further evaluated for their neurotoxicity on P19 NLCs by varying concentrations ranging from 10 μ M to 0.0001 μ M.

The results showed that 17-*O*-ethyl-17-*O*-demethylgeldanamycin (**6**), and 17-*O*-*n*-propyl-17-*O*-demethylgeldanamycin (**8**) exhibited neurotoxicity on P19 NLCs at IC_{50} of 1.6, and 6.7 μ M, respectively and 17-*O*-benzyl-17-*O*-demethylgeldanamycin (**9**), displayed neurotoxicity on P19 NLCs at $IC_{50} > 10.0 \mu$ M. However, 19-*O*-methylgeldanamycin (**18**) showed no neurotoxicity on P19 NLCs ($IC_{50} \gg 10.0 \mu$ M) as shown in Figure 16. Moreover, at very low concentration of 1 nM, all of these four compounds promoted viability of P19 NLCs more than 100%, leading to the observation of the morphology of P19 NLCs treated with compounds **1**, **6**, **8**, **9**, and **18** at concentration of 1 nM under phase-contrast microscope.

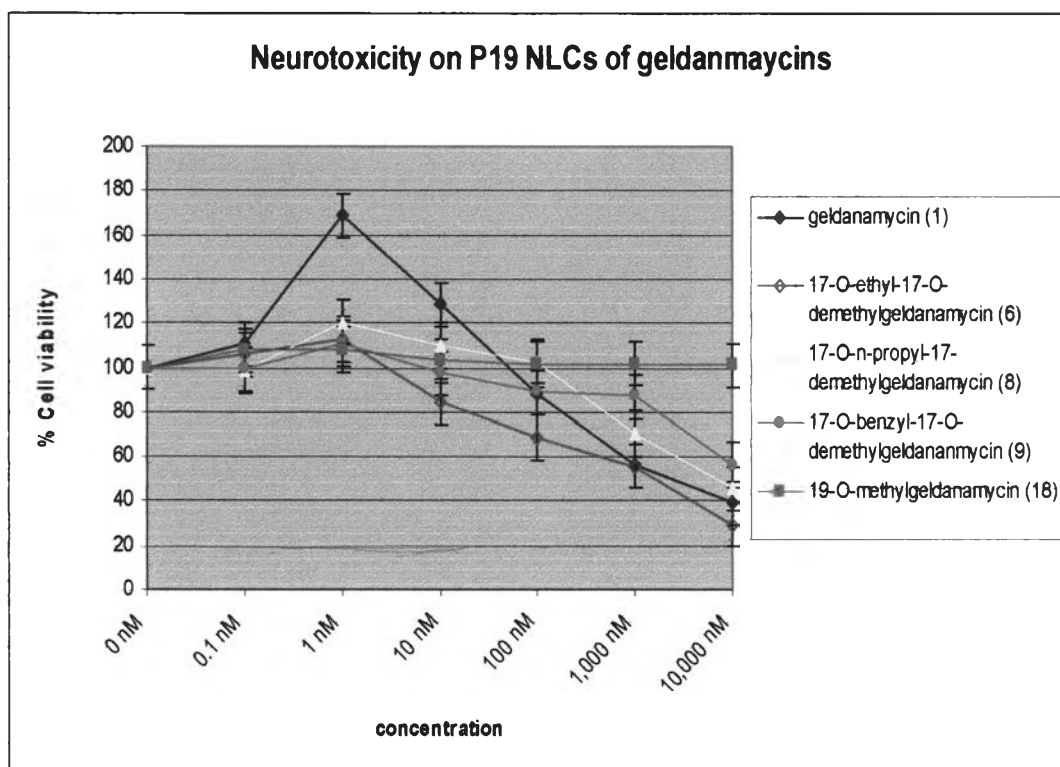


Figure 16. Neurotoxic activity of geldanamycins on P19 NLCs.

The phase-contrast micrographs showed that all of P19 NLCs treated with these compounds exhibited long and/or branching neurites about 2 folds when compared with the control (Figure 17).

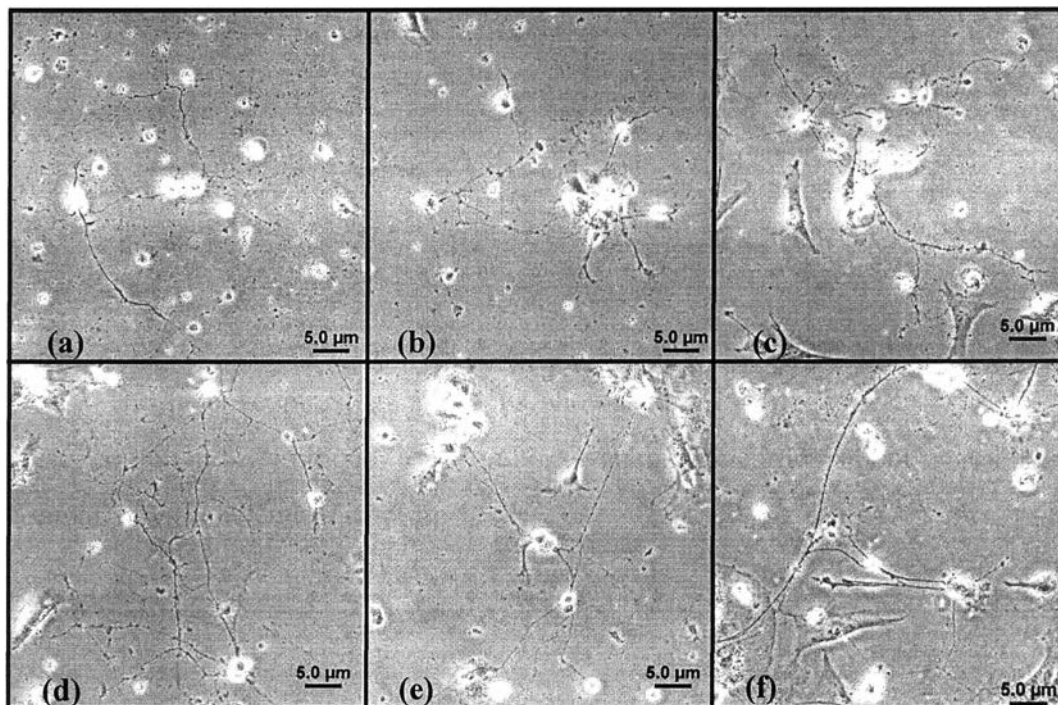


Figure 17. Neuritogenic effects of geldanamycins at 1 nM on P19 NLCs. Phase-contrast micrographs of P19 NLCs cultured for 18 h: (a) control, (b) with geldanamycin (**1**), (c) with 17-*O*-ethyl-17-*O*-demethylgeldanamycin (**6**), (d) with 17-*O*-n-propyl-17-*O*-demethylgeldanamycin (**8**), (e) with 17-*O*-benzyl-17-*O*-demethylgeldanamycin (**9**), and (f) with 19-*O*-methylgeldanamycin (**18**). Bar = 5 μm at 100 \times .

6. Neuroprotective activity of geldanamycins on P19 NLCs

All of the analogues possessed neuritogenic activity included geldanamycin were further evaluated for their neuroprotective ability when co-treated with taxol. First of all, the neurotoxicity dose of taxol on P19 NLCs was investigated. Taxol showed neurotoxicity on P19 NLCs at IC_{50} of 0.65 μM . The neuroprotective ability of neuritogenic geldanamycins were observed. The NLCs were treated with the compounds at concentration of 1 nM together with taxol at concentration of 0.65 μM (Figure 18).

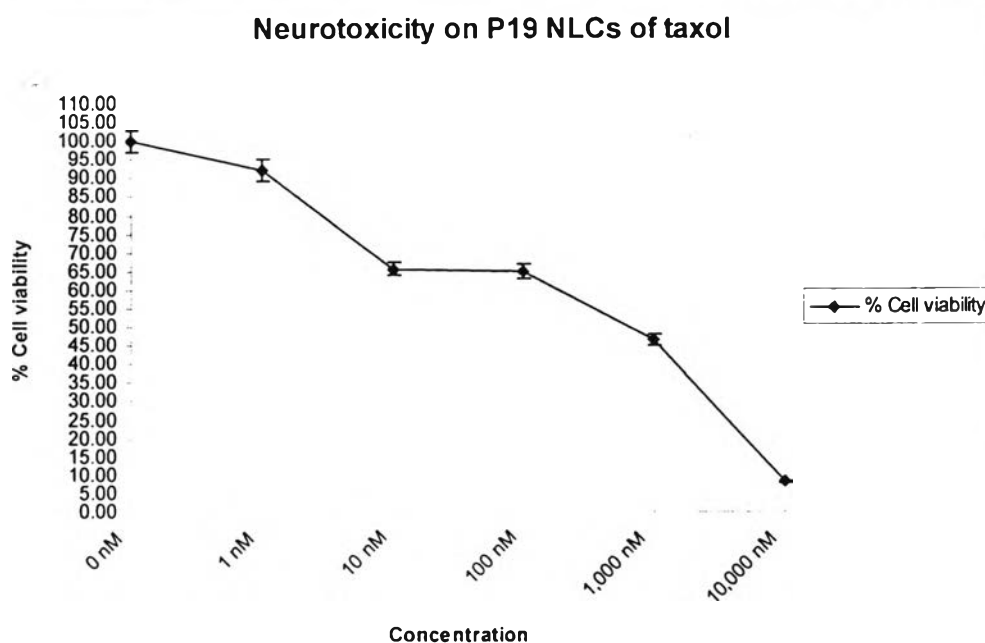


Figure 18. Neurotoxicity of taxol on P19 NLCs ($IC_{50} = 0.65 \mu\text{M}$).

The results observed by XTT reduction assay exhibited that all of the compounds, geldanamycin (**1**), 17-*O*-ethyl-17-*O*-demethylgeldanamycin (**6**), 17-*O*-*n*-propyl-17-*O*-demethylgeldanamycin (**8**), 17-*O*-benzyl-17-*O*-demethylgeldanamycin (**9**), and 19-*O*-methylgeldanamycin (**18**) possessed neuroprotective ability (Figure 19). The percentage of viable P19 NLCs was more than 100% when treated with each compound together with taxol. The neuroprotective ability of these active compounds was further investigated under a phase-contrast microscope by observing the morphology of P19 NLCs treated with these compounds together with taxol at concentration of 1 nM and 0.65 μM , respectively. All of P19 NLCs treated with the compounds together with taxol exhibited long and branching neurites as control while P19 NLCs treated with taxol showed short neurites (Figure 20).

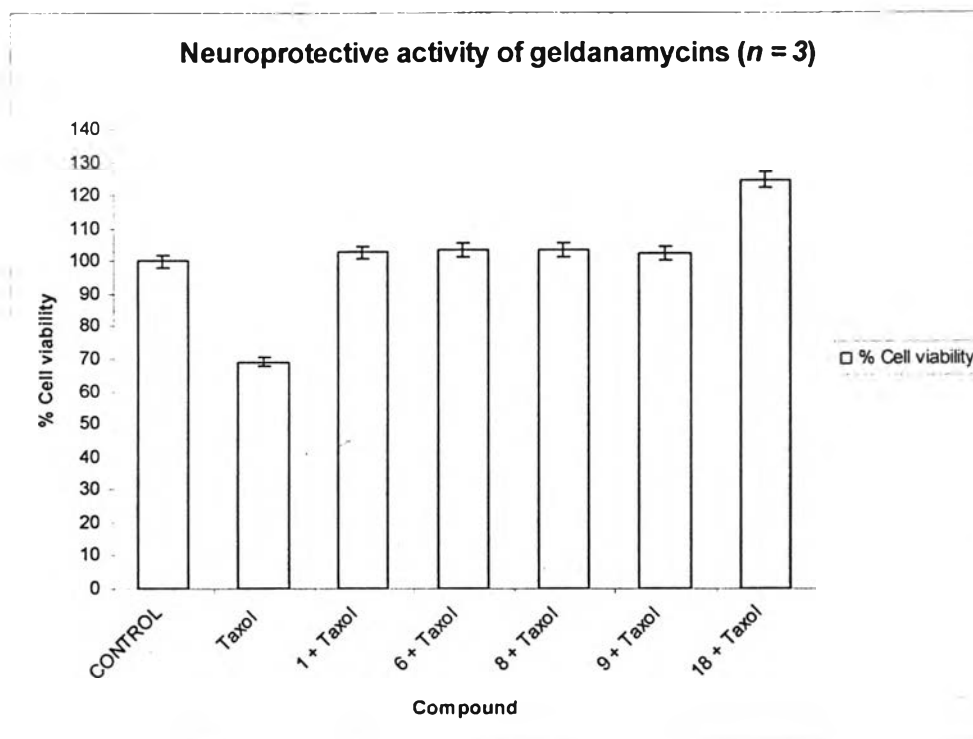


Figure 19. Neuroprotective activity against taxol of geldanamycin and its derivatives on P19 NLCs.

All of the active geldanamycin analogues including geldanamycin itself were evaluated for their therapeutic index (TI). The results were shown in Table 6. Their cytotoxicities on P19 cells were also investigated (Table 6, Figure 21).

Table 6. Biological activities on P19 cells and P19 NLCs of geldanamycin (1), 17-*O*-ethyl-17-*O*-demethylgeldanamycin (6), 17-*O*-*n*-propyl-17-*O*-demethylgeldanamycin (8), 17-*O*-benzyl-17-*O*-demethylgeldanamycin (9), and 19-*O*-methylgeldanamycin (18).

Compound	Cytotoxicity on P19 cells (IC ₅₀)	Neuritogenicity (a) on P19 NLCs	Neurotoxicity (b) on P19 NLCs (IC ₅₀)	TI (b/a)
1	0.1 μM	1 nM	2.0 μM	2,000
6	0.1 μM	1 nM	1.6 μM	1,600
8	0.2 μM	1 nM	6.7 μM	6,700
9	0.5 μM	1 nM	> 10.0 μM	> 10,000
18	> 10.0 μM	1 nM	>> 10.0 μM	>> 10,000

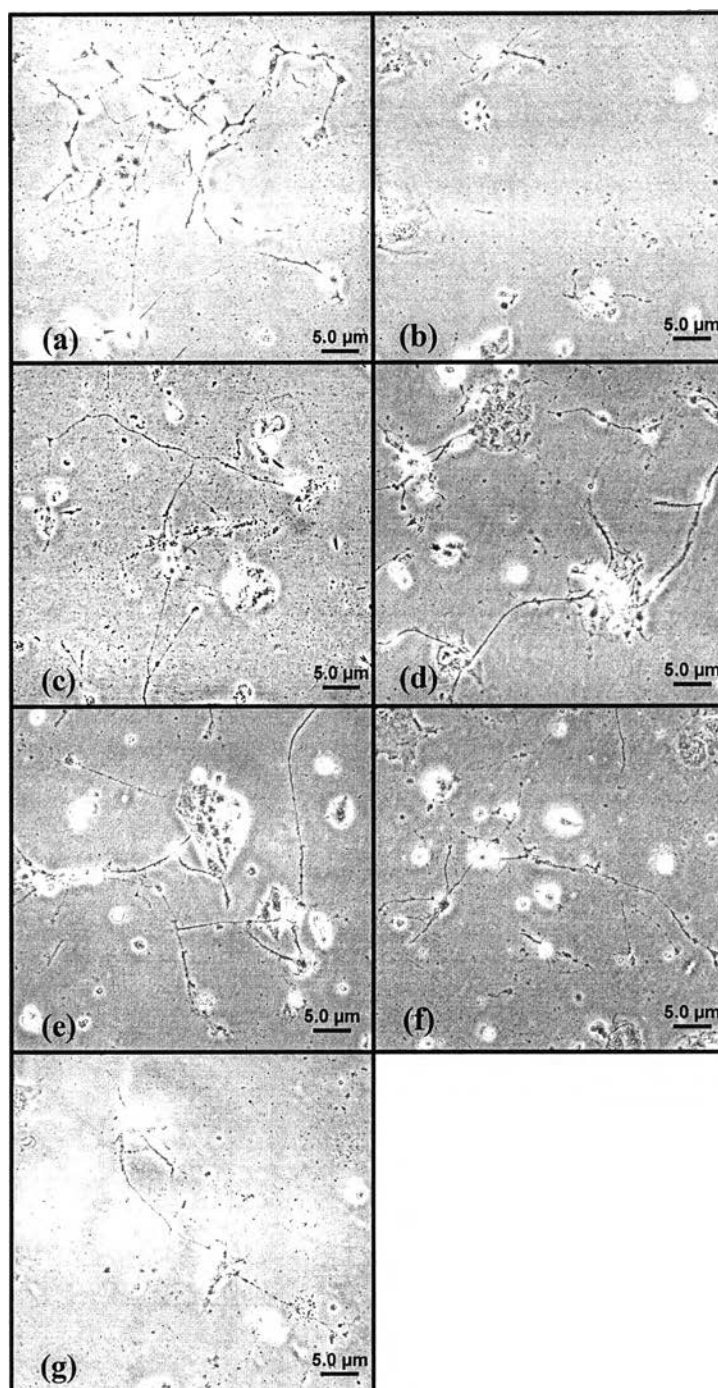


Figure 20. Neuroprotective effects of geldanamycins on P19 NLCs at 1 nM with taxol. Phase-contrast micrographs of P19 NLCs cultured for 18 h: (a) control, (b) with 0.65 μM taxol, (c) with geldanamycin (**1**) and 0.65 μM taxol, (d) with 17-*O*-ethyl-17-*O*-demethylgeldanamycin (**6**) and 0.65 μM taxol, (e) with 17-*O*-*n*-propyl-17-*O*-demethylgeldanamycin (**8**) and 0.65 μM taxol, (f) with 17-*O*-benzyl-17-*O*-demethylgeldanamycin (**9**) and 0.65 μM taxol, and (g) with 19-*O*-methylgeldanamycin (**18**) and 0.65 μM taxol. Bar = 5 μm at 100 \times .

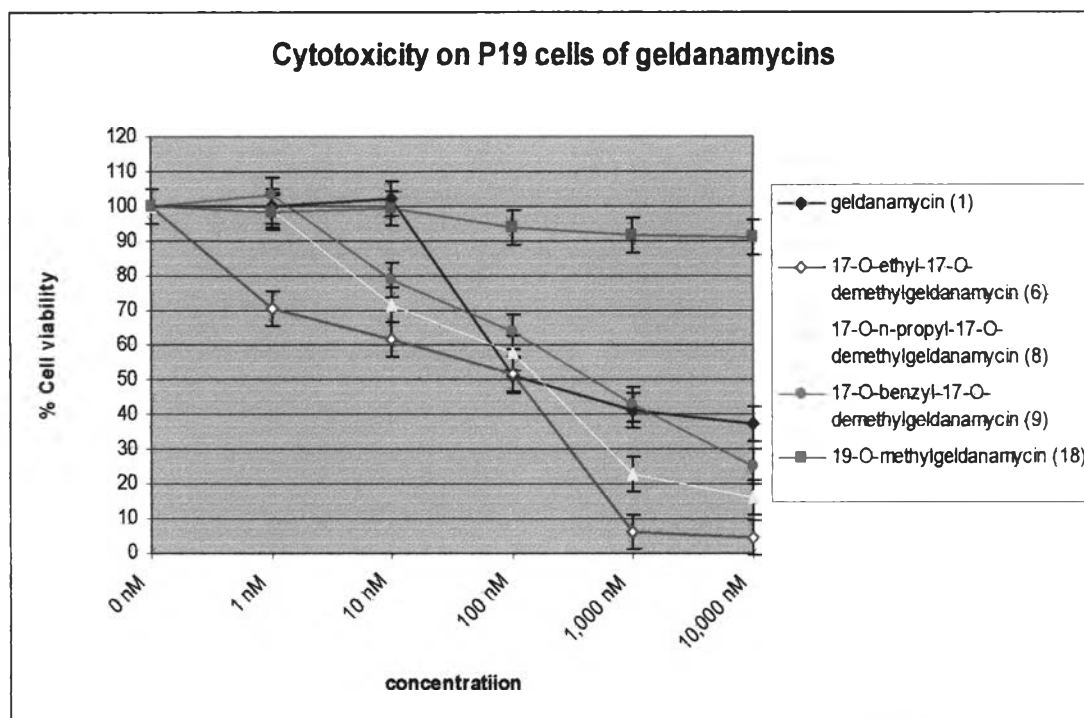
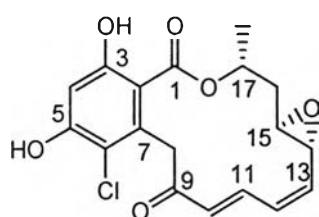


Figure 21. Cytotoxicity of geldanamycins on P19 cells.

According to Table 6, 17-*O*-benzyl-17-*O*-demethylgeldanamycin (9), and 19-*O*-methylgeldanamycin (18) showed the highest therapeutic index in neuritogenic activity and neuroprotective activity. This suggested that longer side chain substituted at C-17 position and substitution at C-19 position which should not longer than methoxy group, reduced the toxicity on P19 NLCs and P19 cells, however, the minimal effective dose of each compound in neuritogenicity and neuroprotective activity should be further investigated because each compound might cause toxicity on other cells.

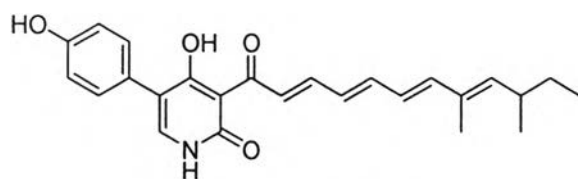
The results mentioned above represented that 19-*O*-methylgeldanamycin (18) and 17-*O*-benzyl-17-*O*-demethylgeldanamycin (9) are notably geldanamycin analogues that possess the remarkably neuritogenic and neuroprotective activities and should be further developed as neuroprotective agents. However, much more 17-*O*-alkyl-17-*O*-demethylgeldamycin analogues should be further synthesized and studied on their biological activities for further development this type of compound as a novel neuroprotective drug.

Some natural products possessed neuritogenic activity such as radicicol (4), an antitumor antibiotic from the fungus *Monosporium bonorden*. Radicicol (4) binds specifically to Hsp90 and acts as an antitumor agent in the similar manner to geldanamycin (1). Treatment of radicicol (4) at 20 nM enhanced the survival and neurite outgrowth of the embryonic sensory neurons from chick embryos. The neuritogenic activity of radicicol (4) was decreased at higher doses. Coadministration of 80 pg/mL (90 pM) of taxol with 20 nM radicicol (4) prevented neurotoxic effect of taxol on the cultures. However, the cellular effect of radicicol (4) is not easily explained. It is presumed that the activity might be mediated via suppression of Hsp90 function (Sano, 2001).

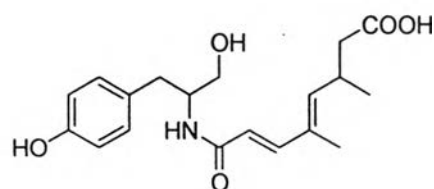


(4)

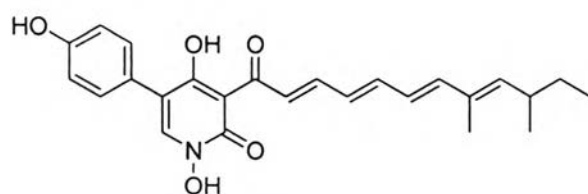
Farinosones A-C (24-26) are the metabolites isolated from mycelial extract of the entomogenous fungal strain *Paecilomyces farinosus* RCEF 0101. Compounds 24 and 26 induced neurite outgrowth in the PC12 cell line at concentration of 50 μ M. All of the compounds showed no cytotoxicity on PC12 cell at 50 μ M concentration in the MTT assay (Cheng *et al.*, 2004).



Farinosone A (24)



Farinosone C (26)



Farinosone B (25)

The neuroprotective substances such as the plant-derived and synthetic cannabinoids affect on cannabinoid receptors, CB₁ receptors, and reduce the release of glutamate and the influx of calcium following the *N*-methyl-D-aspartate (NMDA) receptor activation (Fowler, 2003). The overactivation of glutamate receptors is a major cause of Ca²⁺ overload in cells, potentially leading to cell damage and death. The neuronal damage which occurs as a result of a stroke is largely attributable, not to the immediate hypoxia or ischaemia itself, but to the massive release of glutamate from neurons and glia. Glutamate then activates at least three types of ionotropic receptors, sensitive, respectively, to *N*-methyl-D-aspartate (NMDA), kainite, and α -amino-3-hydroxy-5-methyl-4-isoxazole propionic acid (AMPA). These can all increase the intracellular levels of Ca²⁺ and leads ultimately to the generation of nitric oxide, reactive oxygen species and thus to cell death (Stone and Addae, 2002).

The antioxidants have been recommended for prevention of dementias due to the generation of oxygen free radicals is involved in the pathogenesis of Alzheimer's disease. Alzheimer's disease, a progressive, degenerative disorder of the brain, is the most common cause of cognitive impairment in patients aged ≥ 65 years (Standridge, 2004).

The P19 neuron-like cells contained the GABAergic and cholinergic properties (Jones-Villeneuve *et al.*, 1982; MacPherson and McBurney, 1995; Staines *et al.*, 1994). The cellular response of P19 neuron-like cells caused by neuroprotective agent(s) might resulted from the drug triggers the cells in the pathway(s) mentioned above. However, the action mechanism for neuritogenic and neuroprotective activities of geldanamycins and the cellular response need to be studied. The activities might due to inhibition of activity of Hsp90 because modification at the essential positions for antitumor activity of geldanamycin such as reduction of double bonds at C-2 to C-5 and modification of 11-OH resulting in the loss of neuritogenic activity of geldanamycin. The unrelated cellular effects on P19 cells and P19 neuron-like cells are difficult to explain but might cause from the different phenotypes and cellular response of the different cell types.